Review article Open Access

Tea Andric, Brittany L. Taylor, Katherine E. Degen, Abby R. Whittington, Joseph W. Freeman*

Fabrication and Characterization of Three Dimensional Electrospun Cortical Bone Scaffolds

Abstract: Bone is a composite tissue composed of an organic matrix, inorganic mineral matrix and water. Structurally, bone is organized into two distinct types: trabecular (or cancellous) and cortical (or compact) bone. Cortical bone is highly organized, dense and composed of tightly packed units or osteons whereas trabecular bone is highly porous and usually found within the confines of cortical bone. Osteons, the subunits of cortical bone, consist of concentric layers of mineralized collagen fibers. While many scaffold fabrication techniques have sought to replicate the structure and organization of trabecular bone, very little research focuses on mimicking the organization of native cortical bone. In this study we fabricated three-dimensional electrospun cortical scaffolds by heat sintering individual osteon-like scaffolds. The scaffolds contained a system of channels running parallel to the length of the scaffolds, as found naturally in the haversian systems of bone tissue. The purpose of the studies discussed in this paper was to develop a mechanically enhanced biomimetic electrospun cortical scaffold. To that end we investigated the appropriate mineralization and cross-linking methods for these structures and to evaluate the mechanical properties of scaffolds with varying fiber angles. Cross-linking the gelatin in the scaffolds prior to the mineralization of the scaffolds proved to help prevent channels of the osteons from collapsing during fabrication. Premineralization, before larger scaffold formation and mineralization, increased mineral deposition between the electrospun layers of the scaffolds. A combination of cross-linking and premineralization significantly increased the compressive moduli of the individual scaffolds. Furthermore, scaffolds with fibers orientation ranging between 15° and 45° yielded the highest compressive moduli and yield strength.

Keywords: electrospinning, osteon, cortical, mineralization, force polygon, bone tissue engineering

DOI 10.2478/nanome-2014-0002
Received February 17, 2014; accepted April 15, 2014

***Corresponding author: Joseph W. Freeman:** Rutgers University, Department of Biomedical Engineering, Piscataway, NJ, Tel.: +1 848 445 6595; email: jfreemn@rci.rutgers.edu
Dominion University School of Medical Diagnostic & Translational Sciences, Norfolk, VA 23529, USA

Tea Andric, Abby R. Whittington: Virginia Tech-Wake Forest University, School of Biomedical Engineering and Sciences, Blacksburg, VA, USA 24061
Katherine E. Degen: University of Virginia, Department of Biomedical Engineering, Charlottesville, VA
Abby R. Whittington: Virginia Tech, Material Science and Engineering, Blacksburg, VA
Abby R. Whittington: Virginia Tech, Department of Chemical Engineering, Blacksburg, VA
Brittany L. Taylor: Rutgers University, Department of Biomedical Engineering, Piscataway, NJ

1 Introduction

Bone is a composite tissue composed of organic matrix (20-30 wt %), inorganic bone mineral (60-70 wt %), and water (10 wt%) [1]. Structurally, bone is organized into two distinct types: trabecular (or cancellous) and cortical (or compact) bone. The two types of bone are distinguished by their organization and degree of porosity. Cortical bone is highly organized, dense and compact. It has a low porosity that ranges from 5 to 30% and is usually found on the outside of the bone [2]. Cortical bone is composed of tightly packed units, called osteons, oriented parallel along to the axis of the bone. Osteons are composed of concentric layers of mineralized collagen fibers around a central channel, haversian canal, where vasculature and nerves are housed [3,4,5]. Osteons can range from 100 to 300 µm in diameter [3,4]. The high organization and compact nature of cortical bone provides excellent micro-crack propagation prevention and high tensile and compressive mechanical properties. Trabecular bone is generally found surrounded by cortical bone. It is often referred to as spongy bone, due to an extensive interconnected network of pores, with porosity as high as 90% [2,4,6].

Many fabrication and polymer processing techniques have been investigated for possible bone tissue engineering scaffolds, including sintered microspheres, thermally induced phase separation, particulate leaching, and 3D printing [7-19]. All of the scaffolds are characterized by high porosities, pore interconnectivity, and architectures that mimic the structure of the trabecular bone. Very few fabrication techniques have attempted to create scaffolds that replicate the structural organization of cortical bone.

In a previous study we successfully fabricated electrospun scaffolds which mimicked the structural organization of an osteon [20]. The scaffolds were fabricated by electrospinning onto poly glycolide (PGA) microfibers, which were mounted onto a rotating fiber set up. The resulting scaffolds had diameters within the physiological range of an osteon and were successfully mineralized using 10X simulated body fluid (SBF). A four-week degradation study was performed to degrade the PGA core fibers and create channels, which are naturally found in the osteons; however the PGA fibers did not degrade [20]. To improve upon our earlier work, we sought to fabricate and evaluate three-dimensional scaffolds made from individual osteon-like structures with hollow channels. First, we electrospun scaffolds onto a material that can be easily dissolved out to create biomimetic haversian channels inside of the osteon scaffolds. Next, we utilized a heat sintering technique to combine the individual electrospun osteon-like scaffolds into three-dimensional scaffolds. Scaffolds were mineralized by incubation in 10X SBF and characterized to determine mechanical properties, mineral deposition and distribution. In addition to determining the optimal mineralization and cross-linking procedure, we also discuss the effects of varying the scaffold fiber angle on scaffold compressive strength.

2 Materials and Methods

2.1 Scaffold Fabrication by Electrospinning

Poly(L-lactide) PLLA (inherit viscosity =2.0 dl/g, Mw = 152,000) was chosen as the base scaffold material due to its high tensile strength of 60-70MPa, high tensile modulus of 3GPa, crystalline structure and degradation time (> 24 months) [2, 18]. Poly(D-lactide) (PDLA) (inherit viscosity =102 dl/g, Mw = 124,000) was used to coat the PLLA scaffold to aid with sintering due to its low melting temperature. Poly (ethylene oxide) (PEO) (Mv = 200,000) was used as a space filler that was later dissolved out to mimic the Haversian canal by creating a hollow channel. PLLA, PDLA, and PEO were purchased from Sigma Aldrich (St. Louis, MO, USA).

Dichloromethane (DCM) and dimethylformaldehyde (DMF) were purchased from Fisher Scientific (Pittsburgh, PA, USA). Gelatin, type A, from porcine skin was purchased from Sigma Aldrich (St. Louis, MO, USA). Gelatin, a natural protein derived from denatured collagen, was added to the scaffold to serve as nucleation sites for inorganic precipitation during the mineralization process. The solvents used to create the SBF solution, NaCl, KCl, CaCl $2H_2O$, $MgCl_2$ $6H_2O$, $NaHCO_3$, and NaH_2PO_4, were purchased from Fisher Scientific (Pittsburgh, PA, USA).

PEO was dissolved in a 10% ethanol solution at a concentration of 10% w/v and electrospun onto a rotating 5cm diameter mandrel (~1100rpm) at a rate of 5ml/hr and working distance of 10cm. Total volume of 3ml was electrospun with voltages +10kV and -3kV. The positive voltage was attached to the needle tip while the negative voltage was attached to a wood board covered with foil placed at the opposite side. As the solution is charged, the surface tension of the liquid droplet at the needle tip is overcome by the electrostatic repulsion and the drop is stretched into a thin stream of solid polymer (as the solvent evaporates). The electrospun mats were cut into 3mm wide strips and rolled into thick fibers for electrospinning. Electrospinning solutions were prepared by dissolving 7% w/v PLLA in 75% DCM and 25% DMF, and dissolving 22% w/v PDLA in 75% THF and 25% DMF. The PLLA/gelatin mixture was made by adding 10% w/w dissolved gelatin it to the 7% w/v PLLA solution. To improve immiscibility between the gelatin and PLLA, the solution was vortexed for 1 hour to mix before electrospinning.

Individual osteon-like scaffolds were created by electrospinning PLLA/gelatin and PDLA onto rotating PEO fibers using the set up previously reported, and shown in Figure 1 [18]. PLLA/gelatin mixture was first electrospun unto the thick PEO fiber to a total volume of 1.5ml, with the following parameters: working distance of 5cm, pump rate of 5ml/hr, and voltages of + 17kV and -9kV. This was followed by electrospinning a total volume of 0.5ml of the PDLA solution onto the PLLA/gelatin wrapped PEO fibers with the following parameters: working distance of 15cm, pump rate of 5ml/hr, and voltages of +13kV and -8kV.

Finally, PLLA/gelatin/PDLA sheets were created by electrospinning 1ml of PDLA followed by 5ml of PLLA/gelatin solution onto a 5cm diameter rotating mandrel (~2000rpm). The electrospun mats were cut into 1cm wide strips and later used in the heat sintering process to combine the osteon-like scaffolds previously mentioned. All electrospun scaffolds were cross-linked in 2.5% glutaraldehyde vapor for either 2 hours or 17 hours.

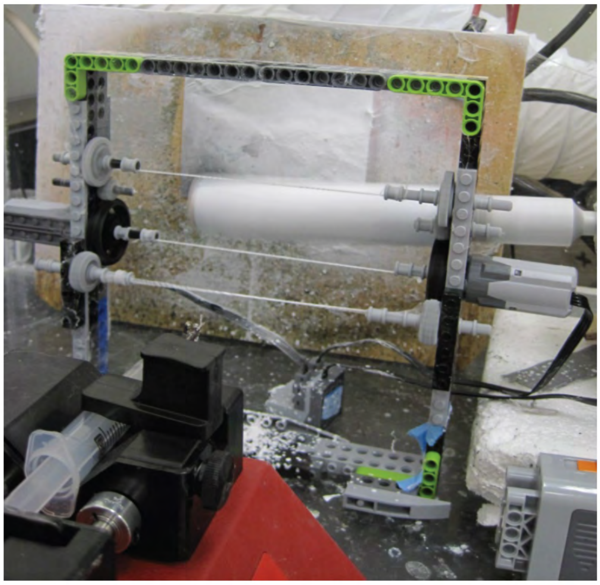

Figure 1: Picture of the electrospinning set-up for rotating PEO fibers.

2.2 Heat sintering of the Scaffolds

Three-dimensional electrospun scaffolds were fabricated utilizing a heat sintering method previously reported by our group [21]. Individual osteon-like scaffolds were cut into 1cm segments and wrapped with 1cm wide strip of the electrospun PLLA/gelatin/PDLA sheet to a diameter of 5mm. The wrapped scaffolds were then placed into a mold (5mm diameter with 1cm height) and heat sintered at 54°C for 45 minutes.

2.3 Mineralization of the Scaffolds

All scaffolds were mineralized using a previously reported method by incubation in 10X SBF [22,23]. Briefly, a stock solution was made by dissolving NaCl, KCl, CaCl x $2H_2O$, $MgCl_2$ x $6H_2O$, and NaH_2PO_4 in dI H_2O and stored at room temperature. Prior to the mineralization process, $NaHCO_3$ was added while stirring vigorously, resulting in the following ion concentrations: Ca^{2+} 25mM, HPO_4^{2-} 10mM, Na^+ 1.03M, K^+ 5mM, Mg^{2+} 5mM, Cl^- 1.065M, and HCO_3^- 10mM and a pH of about 4.4. The electrospun scaffolds were incubated in 300ml of 10X SBF for various times at room temperature. The mineralization solution was replaced every 2 hours. After being removed from 10X SBF, all the samples were rinsed in dI water to remove mineral not attached to scaffolds, and vacuum dried overnight.

For the scaffolds with premineralization treatment, individual osteons and electrospun sheets were mineralized for 1 hour, rinsed in dI water and vacuum dried overnight. The electrospun pieces were then heat sintered as described above and mineralized again as a combined three- dimensional scaffold.

2.4 Alizarin Red Staining

Mineral deposition and distribution was characterized using Alizarin red stain. The scaffolds were fixed in 70% ethanol for 1hr at 4°C, and stained with 40mM Alizarin red solution for 10 min. The scaffolds were then washed with dI water, placed into cryomolds, imbedded in OCT imbedding medium, and frozen at -20°C. The scaffolds were cut into 200µm section using a Cryostat HM 550 (Thermo Scientific Microm, Walldorf, Germany), and imaged using stereoscope (Vision Engineering, New Milford, CT, USA).

2.5 Scaffold Fabrication with Varying Fiber Angles

PLLA/gelatin/PDLA electrospun mats were created as previously discussed and were placed above a 25mM solution glutaraldehyde for two hours for vapor crosslinking. Strips 1cm wide were cut at varying angles from the top right corner of the scaffold. The sample groups where angled strips cut at 0°, 15°, 30°, 45° and 90° (Figure 2). This is based on the assumption that the nanofibers were aligned after formation. The strips were then wrapped around a 18 gauge blunt needle tip and heat sintered at 54°C for 45 minutes to create three-dimensional electrospun columns with average diameters of .5cm and 1cm in height.

2.6 Mechanical Testing

The scaffolds were mechanically tested in compression using an Instron 5869 with Bioplus Bath (Norwood, MA, USA). Scaffolds tested included: Mineralized scaffolds (Min) for 6 and 24 hours, cross-linked scaffolds for 2h (CL) and mineralized for 6hr, scaffolds premineralized for 1 hr without cross-linking (premin1h), scaffolds cross-linked for 2 hours and premineralized (CL_premin1hr) and then mineralized for 6 and 24 hours, and the scaffolds with varying fiber angles. For each group we tested six samples (n=6). The tests were performed under simulated physiological conditions in phosphate buffered saline (PBS) (pH= 7.4) at 37°C. The scaffolds were fabricated into 10mm high cylinders with 5mm diameter (2:1 height to diameter ratio) and tested in compression until failure with uniform strain rate of 1mm/min (10% stain/min). The data was analyzed to determine yield stress and compressive modulus.

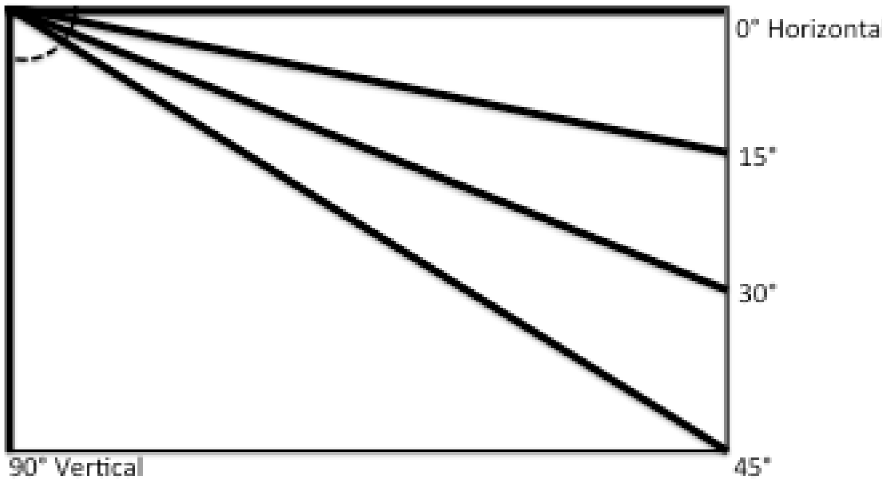

Figure 2: Diagram of strips cut at varying fiber angles.

2.7 Mineral Ash Weights

To quantify the amount of inorganic mineral on the scaffolds, mineral ash weights were determined. After the initial weight of the samples was recorded, the samples were placed in ceramic crucibles, and then placed into a high temperature furnace (Model No. FD1535M, Fisher Scientific, Pittsburgh, PA, USA) at 700°C for 24 hr. After cooling down, the mineral ash weight was recorded and the average mineral percent deposition calculated as ratio of mineral ash weight to samples original weight. For each group we tested three samples (n=3).

2.8 Statistical Analysis

Statistical analysis was performed using JMP 9 software. All the data was analyzed using one-way analysis of variance (ANOVA) with Tukey's test to determine statistically significant differences between groups. Statistical significance was tested at $p < 0.05$.

3 Results

In this study, the objective was to create hollow, tubular scaffolds. In order to accomplish this we electrospun nanofibers onto an easily dissolvable material to create channels. The purpose of the hollowed channels was to mimic haversian canals where the bone vasculature is housed. PEO fibers created from an electrospun mat were used as core fibers in our rotating set up (Figure 1) to fabricate osteon-like scaffolds. We initially soaked individual scaffolds, which revealed that PEO would completely dissolve out but cause the hollow center of the osteon scaffolds structures to collapse. To prevent the scaffold channels from collapsing, individual osteon-like scaffolds were combined and heat sintered into 3D scaffold and then cross-linked. Once the scaffolds were sintered, the PEO fibers could then be dissolved out leaving a set of channels running along the length of scaffolds; mimicking the organization of the cortical bone.

3.1 Alizarin Red Staining

Alizarin red staining was used to stain the mineral deposited on the scaffolds. A majority of the mineral can be seen on the outer most layers of the scaffolds. The mineralization process of soaking in 10X SBF dissolved out PEO core fibers from individual osteons, leaving behind a system of channels that run along the length of the scaffolds. Premineralization treatment, without cross-linking of the scaffolds, resulted in the dissolution of PEO cores and collapse of the individual osteon–like scaffolds, as shown in Figure 3B. Cross-linking the osteons prior to the premineralization treatment kept the individual osteons open without collapsing, thus preserving the channels (Figure 3C and D) and allowing mineralization to take place inside of the channels (Figure 3). The scaffolds that were premineralized, crosslinked and mineralized for 6 hours (Figure 3D) and 24 hours (Figure 3F) had the most mineral deposition. Furthermore, the scaffolds mineralized for 24 hours after premineralization and cross-linked had higher mineral deposition than mineralized scaffolds without any treatment (Figure 3E).

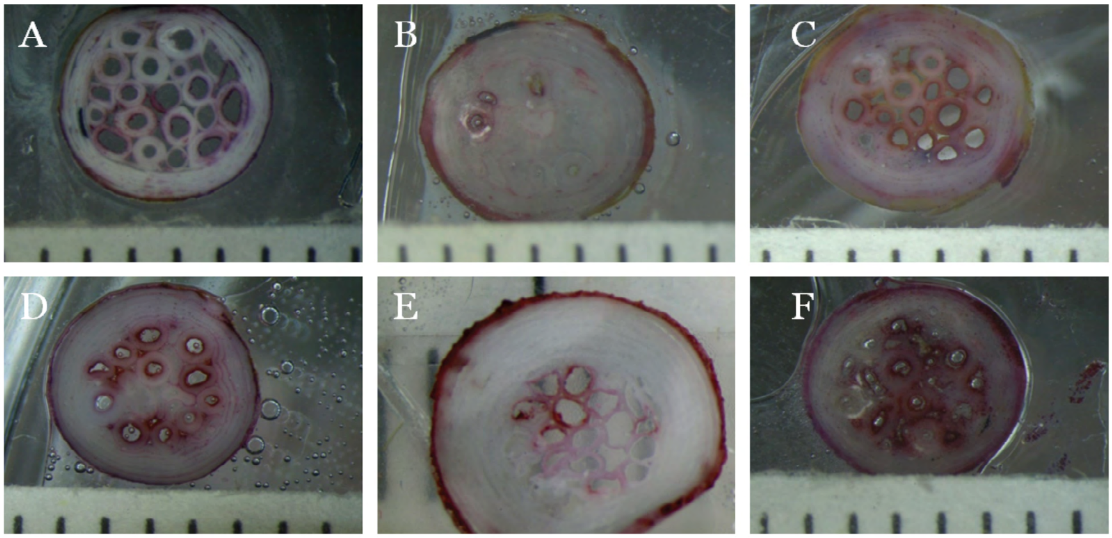

Figure 3: Alizarin red stain of cross-sections after 6hr (A-C) and 24hr (E, F) mineralization process: A) Min6h, B) Premin1h_Min6h, C) CL_Min6h, D) CL_premin1h_Min6h, E) Min24h, and F) CL_premin1h_Min24h. Statistical significance proven using ANOVA Tukey Test (post-hoc) $p<0.05$.

3.2 Mechanical Testing

The compressive mechanical properties of the scaffolds were also evaluated using an Instron 5869. In the first study, the compressive moduli and compressive yield stresses of scaffolds with varying cross-linking and mineralization methods was compared, as shown in Figure 4 and 5. After 24 hours of mineralization, the premineralized cross-linked scaffolds had significantly higher compressive moduli than the mineralized (6hr and 24hr) scaffolds and premineralized only (6hr) scaffolds. A similar trend is seen with the 6 hours of mineralization study. The premineralized cross-linked scaffolds had significantly higher compressive moduli than the premineralized only scaffolds.

Scaffolds mineralized only for 6 hours and 24 hours and cross-linked for 6 hours scaffolds had significantly higher yield stresses than scaffolds that were premineralized first. Also, the cross-linked and mineralized for 6 hours only scaffolds had significantly higher yield stresses than scaffolds that were cross-linked and then premineralized.

Figures 6 and 7 show the compressive moduli and compressive yield stresses for the scaffolds with varying fiber angles (0°, 15°, 30°, 45°, 90°). The samples with 0° and 90° angled fibers had the lowest yield stress and young's modulus whereas the samples with the angled fibers at 15°, 30° and 45°, displayed a higher compressive modulus and yield stress. Also, a decreasing trend is seen with the 15°, 30°, and 45° angled fibers. As the fiber angles increased from 15° to 45°, the compressive modulus and compressive yield strengths decreased.

3.3 Mineral Ash Weights

Mineral ash weights were determined to quantify the amount of mineral present on the scaffolds. Two groups of scaffolds were analyzed: mineralized only and cross-linked then premineralized scaffolds. Two mineralization times, 6hr and 24hr, were investigated. Mineral ash weighs of the scaffolds were recorded and shown in Table 1. The combination of cross-linking and premineralization treatment resulted in a significant increase in mineral deposition both after 6 and 24 hours of mineralization. Mineral deposition increased with increased mineralization time, as expected.

4 Discussion

This study was a follow up to our previous study where we successfully fabricated scaffolds that mimicked individual osteons found in cortical bone [20]. In the previous study, scaffolds were fabricated by electrospinning onto poly glycolide (PGA) microfibers and consisted of concentric layers of electrospun fibers surrounding a PGA core. The

Table 1: Mineral ash weight percentages.

Group	% ash weight
CL_Min 6h	2.89%
Min 6h	2.59% ± 0.003
Min 24h	9.78% ± 0.015
Premin 1h_Min6h	7.48%
CL_premin_Min6h	5.10%

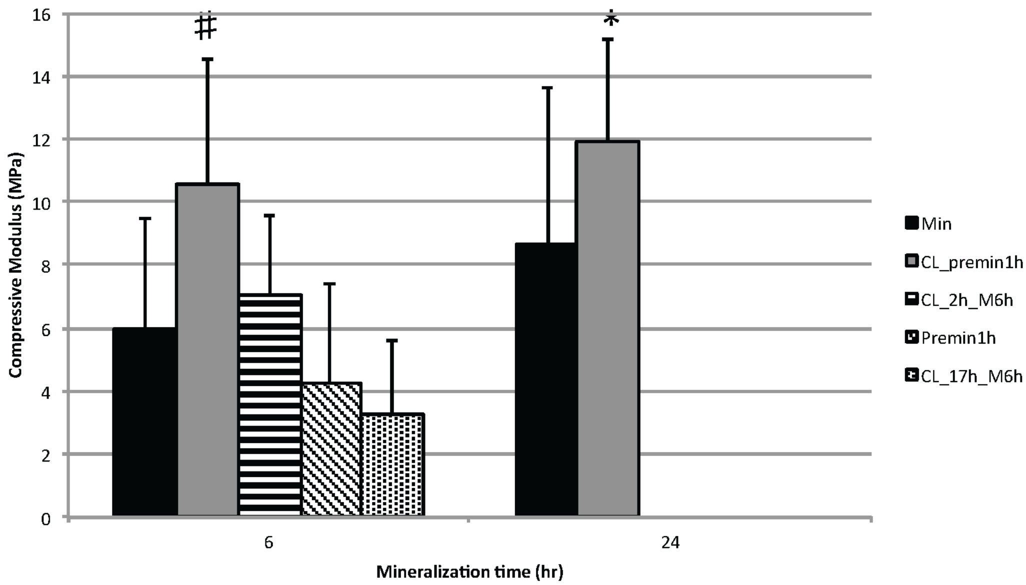

Figure 4: Compressive moduli of scaffolds. * - from Min_24h, # - from Premin1h, Min6hr and CL_17hr_Min6hr. Statistical significance proven using ANOVA Tukey Test (post-hoc) $p<0.05$.

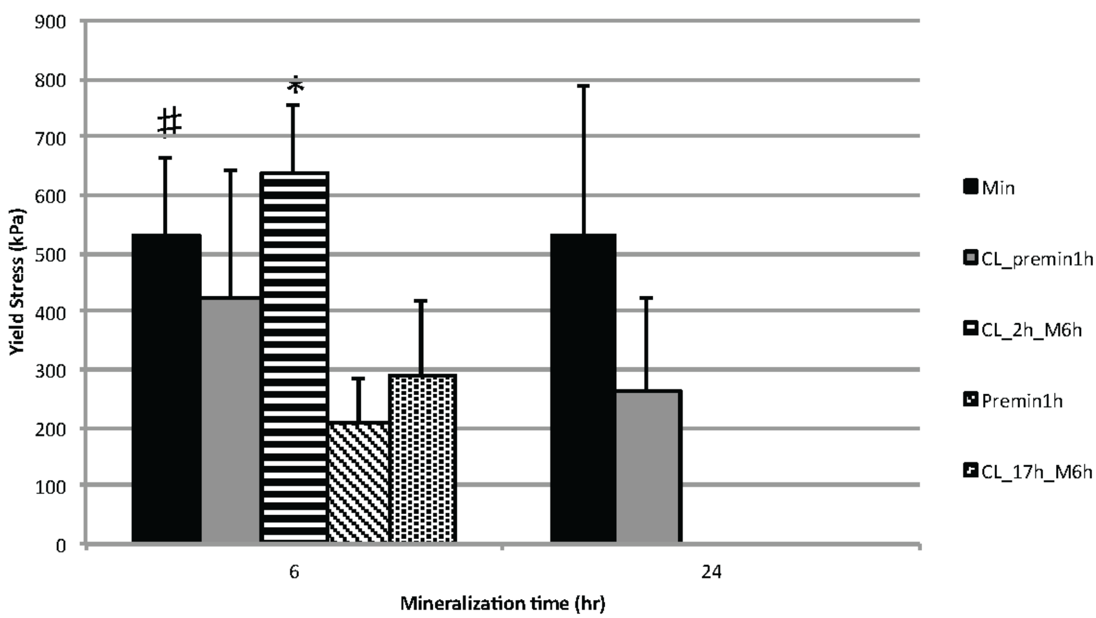

Figure 5: Compressive Yield Strength of scaffolds. *-from Min_24h, #-from Premin1h, Min6hr and CL_17hr_Min6hr. Statistical significance proven using ANOVA Tukey Test (post-hoc) $p<0.05$.

scaffolds were also biocompatible, as they supported cell attachment, proliferation and also mineral deposition over the period of 4 weeks. However, a 4-week degradation study concluded PGA core fibers did not degrade [20]. The lack of core fiber degradation would prevent the formation of the hollow channels, which are naturally found in the osteons. These natural channels, Haversian canals, are necessary for cellular and nutrient movement and future development of vasculature.

In the present study we electrospun around a hydrophilic polymer composed of PEO to create a hollow channel within the electrospun osteon-like scaffolds. The individual electrospun osteon-like scaffolds were combined together and heat sintered into 3D scaffolds to mimic the organization of cortical bone. Mineralization by incubation in 10X SBF dissolved away the PEO core fiber, leaving behind a system of channels that run along the length of the scaffolds, similar to native haversian canals.

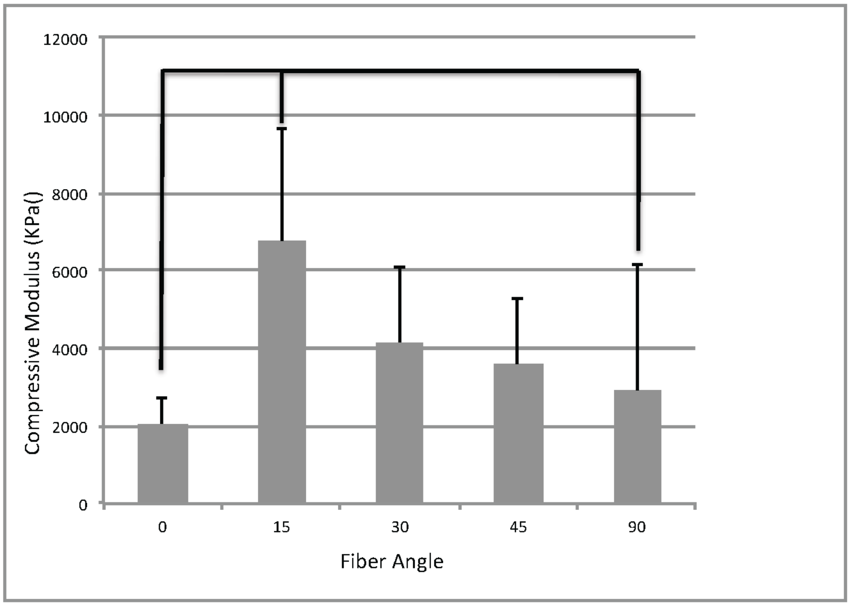

Figure 6: Compressive Moduli of scaffolds with varying fiber angles. Columns with fibers angled at 15° was significantly greater than the columns with 0° and 90° angled fibers. Statistical significance proven using ANOVA Tukey Test (post-hoc) p<0.05.

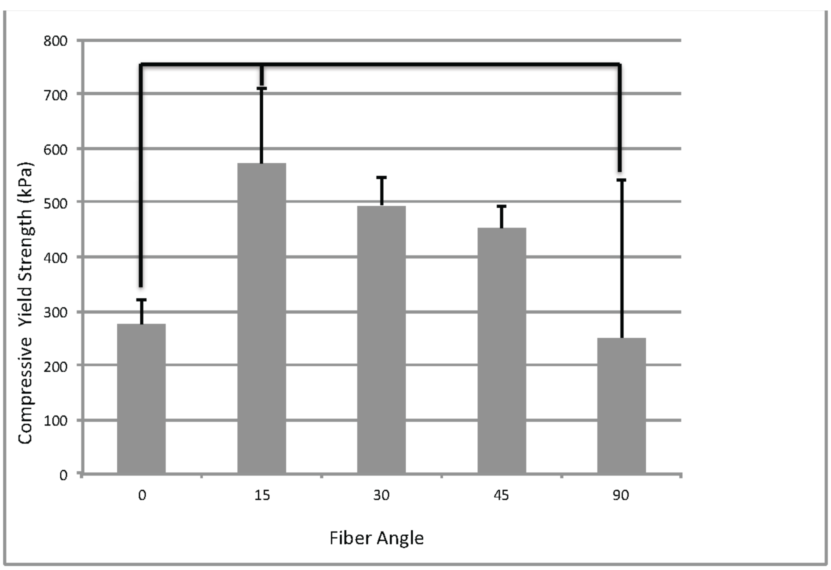

Figure 7: Compressive Yield Strength of scaffolds with varying fiber angles. Columns with fibers angled at 15° was significantly greater than the columns with 0° and 90° angled fibers. Statistical significance proven using ANOVA Tukey Test (post-hoc) p<0.05.

Cross-linking of the gelatin prior to the mineralization of the scaffolds prevented the hollow channels within the osteons from collapsing during dissolution of PEO fibers. A premineralization treatment was introduced consisting of mineralizing all individual osteon scaffolds and electrospun mats for 1 hour, prior to heat sintering. The goal was to introduce mineral particles to serve as seeds once the scaffolds are heat sintered into 3D structures. However, the premineralization treatment resulted in the dissolution of PEO and collapse of the channels in the scaffolds. Cross-linking the gelatin prior to the premineralization treatment kept the channels open and allowed mineral deposition on the inside of the channels (Figure 3D). The combination of premineralization and cross-linking treatments resulted in better mineral distribution inside the channels of the scaffolds and more mineral overall compared to just mineralization alone, both after 6 hour and 24 hour of mineralization. The amount of mineral deposited was quantified by determining mineral ash weights of the scaffolds. While increased mineralization time increased mineral deposition, the combination of premineralization and cross-linking resulted in a more significant increase in mineral deposition.

We also evaluated the compressive mechanical properties of the scaffolds after different mineralization and cross-linking treatments. Cross-linking of gelatin combined with premineralization significantly increased compressive moduli over mineralization alone after 24 hours and over premineralization alone, after 6 hours of mineralization. The purpose of this study was to determine which crosslinking method, premineralization, and mineralization time would yield the greatest mechanical properties. Therefore, we did not include the groups that displayed weaker mechanical properties (CL_17hr_M6h, CL_2hr_M6h, and Premin1h) in the 24hr mineralization study as seen in Figures 4 and 5.

Premineralization may affect the mechanics by increasing the overall amount of mineral in the scaffolds and also improving the distribution, as seen in the alizarin red stains. However, the presence of mineral can interfere with binding of layers during the heat sintering process. Cross-linking of the gelatin may also contribute to the increase in scaffold mechanical strength. Gelatin is water soluble, and without cross-linking process can be dissolved and lost from the scaffolds [22-24]. Electrospun gelatin is commonly cross-linked in glutaraldehyde vapor, which is also a commonly used cross-linking method for electrospun collagen. The vapor glutaraldehyde cross-linking occurs between the carboxyl groups on the glutaraldehyde and the amine groups of the gelatin [24]. Gelatin was also found to increase tensile mechanical properties of the electrospun scaffolds. The cross-linking process preserves the gelatin and may contribute to mechanical properties of the scaffolds.

Differences in scaffold compressive mechanical properties with varying fiber angles were also evaluated. The purpose of this study was to determine a nanofiber angle within the scaffold, which would yield the highest compressive mechanical properties. The electrospun scaffolds were cut into strips s and rolled at various angles into columns. The differences in mechanical behavior as a result of varying the fiber angle can be explained using the force polygon shown in Figure 8A. The force polygon depicts the forces acting internally within each column [25]. The angle from the upright origin (β) is the corresponding angle at which the strips were cut: 0°, 15°, 30°, 45° and 90°. The total forces, horizontal, vertical and an inclined internal, collectively add to the increased yield strength and young's modulus of the columns. This is evident in the decreased mechanical properties of the columns with 0° and 90° angled fibers. The columns with the 0° angled fibers do not have a horizontal force, therefore decreasing the overall total force. The columns with the 90° angled fibers lack a horizontal or internal inclined forces and therefore yielded the lowest total forces of all the fibers (cos 0° = tan 0° = 0) and hence, the lowest compressive mechanical properties.

The axial forces within the columns defined as the inclined forces, N, are equal to the combination of a vertical (gravity loads) and horizontal component. The horizontal component is a result of the angle and inclined internal force and the vertical component is the known yield strength exerted by the column. From the force polygon, the relationship between the inclined internal force, the vertical force and horizontal force are shown the equations in Figure 8B. The mechanical properties of the columns correspond to the fibers acting as individual forces, which oppose the applied compressive load. As a results, the angled fibers at 15°, 30°, and 45° had greater total forces, vertical, horizontal, and inclined internal forces, acting against compression thus yielding higher mechanical strength.

5 Conclusion

In this study we successfully fabricated three dimensional electrospun scaffolds composed of heat sintered individual osteon-like scaffolds. The scaffolds contained a system of hollow channels running parallel to the length of the

A

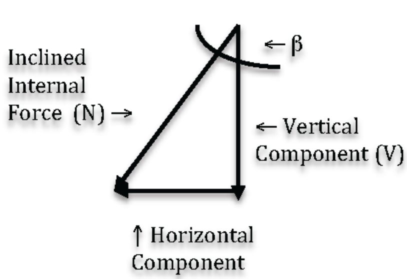

B

$$\frac{V}{N} = \cos\beta \rightarrow \qquad N = \frac{V}{\cos\beta}$$

$$\frac{H}{V} = \tan\beta \rightarrow \qquad H = V\tan\beta$$

Figure 8: A) Force polygon, B) Force polygon equations

scaffolds, as found naturally in the haversian systems of bone tissue. Cross-linking of the gelatin in the scaffolds prior to mineralization helped prevent the channels within the osteons from collapsing during dissolution of the PEO core fibers. The combination of cross-linking and premineralization significantly increased the overall amount of mineral and mineral distribution in the scaffolds, and also improved compressive moduli of the scaffolds. Furthermore, we conclude that scaffolds with angled fibers ranging from 15° to 45° yielded greater mechanical strength. The angled fibers act as opposing vertical, horizontal, and inclined internal forces, which sum up to the total force being exert by the scaffold columns. These scaffold fabrication techniques will be utilized further to fabricate scaffolds that mimic the dual structural organization and mechanical properties of natural bone with cortical and trabecular regions.

Conflict of interest statement: Authors state no conflict of interest.

References

[1] Chen, J.; Chu, B.; Hsiao, B. S., Mineralization of hydroxyapatite in electrospun nanofibrous poly(L-lactic acid) scaffolds. *J Biomed Mater Res A* 2006, *79* (2), 307-17.

[2] An, Y. H.; Woolf, S. K.; Friedman, R. J., Pre-clinical in vivo evaluation of orthopaedic bioabsorbable devices. *Biomaterials* 2000, *21* (24), 2635-52.

[3] Ritchie, R. O., How does human bone resist fracture? *Ann N Y Acad Sci 2010, 1192* (1), 72-80

[4] Rho, J. Y.; Kuhn-Spearing, L.; Zioupos, P., Mechanical properties and the hierarchical structure of bone. *Med Eng Phys* 1998, *20* (2), 92-102

[5] Beniash, Elia. “Biominerals—hierarchical nanocomposites: the example of bone.” *Wiley Interdisciplinary Reviews: Nanomedicine and Nanobiotechnology, 2011,* 3 (1), 47-69

[6] Cowin, S. C.; Doty, S. B., *Tissue mechanics*. Springer: New York, NY, 2007; p xvi, 682 p.

[7] Borden, M.; El-Amin, S. F.; Attawia, M.; Laurencin, C. T., Structural and human cellular assessment of a novel microsphere-based tissue engineered scaffold for bone repair. *Biomaterials* 2003, *24* (4), 597-609

[8] Borden, M.; Attawia, M.; Khan, Y.; Laurencin, C. T., Tissue engineered microsphere-based matrices for bone repair: design and evaluation. *Biomaterials* 2002, *23* (2), 551-9.

[9] Wei, G.; Ma, P. X., Structure and properties of nano-hydroxy-apatite/polymer composite scaffolds for bone tissue engineering. *Biomaterials* 2004, *25* (19), 4749-57

[10] Wang, X.; Song, G.; Lou, T., Fabrication and characterization of nano composite scaffold of poly(L-lactic acid)/hydroxyapatite. *J Mater Sci Mater Med, 2009, 21*(1), 183-8

[11] Ma, P. X.; Zhang, R., Microtubular architecture of biodegradable polymer scaffolds. *J Biomed Mater Res* 2001, *56* (4), 469-77.

[12] Lu, L.; Peter, S. J.; Lyman, M. D.; Lai, H. L.; Leite, S. M.; Tamada, J. A.; Uyama, S.; Vacanti, J. P.; Langer, R.; Mikos, A. G., In vitro and in vivo degradation of porous poly(DL-lactic-co-glycolic acid) foams. *Biomaterials* 2000, *21* (18), 1837-45

[13] Chen, V. J.; Ma, P. X., Nano-fibrous poly(L-lactic acid) scaffolds with interconnected spherical macropores. *Biomaterials* 2004, *25* (11), 2065-73.

[14] Yang, S.; Leong, K. F.; Du, Z.; Chua, C. K., The design of scaffolds for use in tissue engineering. Part I. Traditional factors. *Tissue Eng* 2001, *7* (6), 679-89

[15] Stevens, B.; Yang, Y.; Mohandas, A.; Stucker, B.; Nguyen, K. T., A review of materials, fabrication methods, and strategies used to enhance bone regeneration in engineered bone tissues. *J Biomed Mater Res B Appl Biomater* 2008, *85* (2), 573-82

[16] Rezwan, K.; Chen, Q. Z.; Blaker, J. J.; Boccaccini, A. R., Biodegradable and bioactive porous polymer/inorganic composite scaffolds for bone tissue engineering. *Biomaterials* 2006, *27* (18), 3413-31

[17] Liu, X.; Ma, P. X., Polymeric scaffolds for bone tissue engineering. *Ann Biomed Eng* 2004, *32* (3), 477-86.

[18] Andric, T.; Sampson, A. C.; Freeman, J. W., Fabrication and characterization of electrospun osteon mimicking scaffolds for bone tissue engineering. *Materials Science & Engineering C-Materials for Biological Applications* 2011, *31* (1), 2-8

[19] Wright, L. D.; Young, R. T.; Andric, T.; Freeman, J. W., Fabrication and mechanical characterization of 3D electrospun scaffolds for tissue engineering. *Biomed Matre, 2010, 5*(5), 055006

[20] Andric, T.; Wright, L. D.; Freeman, J. W., Rapid Mineralization of Electrospun Scaffolds for Bone Tissue Engineering. *J Biomater Sci Polym Ed, 2011, 22(11), 1535-1550*

[21] Tas, A. C.; Bhaduri, S. B., Rapid coating of Ti6A14V at room temperature with a calcium phosphate solution similar to 10x simulated body fluid. *Journal of Materials Research* 2004, *19* (9), 2742-2749

[22] Heydarkhan-Hagvall, S.; Schenke-Layland, K.; Dhanasopon, A. P.; Rofail, F.; Smith, H.; Wu, B. M.; Shemin, R.; Beygui, R. E.; MacLellan, W. R., Three-dimensional electrospun ECM-based hybrid scaffolds for cardiovascular tissue engineering. *Biomaterials* 2008, *29* (19), 2907-14

[23] Sisson, K.; Zhang, C.; Farach-Carson, M. C.; Chase, D. B.; Rabolt, J. F., Fiber diameters control osteoblastic cell migration and differentiation in electrospun gelatin. *J Biomed Mater Res A, 2010, 94* (4), 1312-24

[24] Sisson, K.; Zhang, C.; Farach-Carson, M. C.; Chase, D. B.; Rabolt, J. F., Evaluation of cross-linking methods for electrospun gelatin on cell growth and viability. *Biomacromolecules* 2009, *10* (7), 1675-80